ABSTRACT

DILLARD, LUCAS BRUCE. Understanding the Kinetic and Thermodynamic Properties of the Thermophilic Oxoglutarate Carboxylase (Under the direction of Dr. Robert B. Rose).

For many biofuel crops, carbon fixation is limiting –making the production of these alternative fuels economically unviable. The first green revolution has led to significant advances in crop yields in the past half century. Today, crop yield is now mostly limited by plant biology and to overcome this limitation, a condensed reverse tricarboxylic acid (crTCA) cycle has been designed in the workhorse species *Camelina sativa* that fixes dissolved carbon dioxide. The biotin-dependent carboxylase Oxoglutarate Carboxylase (OGC) presents itself as the slow step of the crTCA cycle engineered in *Camelina sativa.* OGC –a thermophile –is 500-fold less active at mesophilic temperatures than at its optimal 76 ℃. Engineering OGC to preserve high activity at mesophilic temperatures presents an opportunity to further improve the rate of carbon fixation in the crTCA pathway, and possibly increase yields in oil seed crops, –reducing the cost of biofuels.

Biotin-dependent carboxylases such as OGC are a ubiquitously found family of proteins that consist of three domains: The Biotin Carboxylase (BC) domain, Biotin Carboxyl Carrier Protein (BCCP), and the Carboxy Transferase (CT) domain. The BC domain of OGC has been chosen to study first, because of the availability of highly similar mesophilic paralogs. I report kinetic ATPase activity measurements of the thermophilic OGC BC domain measured via discontinuous assay coupled with direct quantitation of ADP production via High Performance Liquid Chromatography (HPLC). ATP concentration dependent activity was observed at temperatures ranging

from 49℃ to 76℃, with k_{cat} at 76℃ being 79 min^{-1}. A subsequent Eyring plot was generated to measure the free energy of the transition state of OGC BC and determined $\Delta G^{\ddagger}$, $\Delta H^{\ddagger}$, and $\Delta S^{\ddagger}$ to be 17.4 ± 1.3 kcal/mol, 13.7 ± 1.3 kcal/mol, and 11 ± 4 Cal/mol*K, respectively. Subsequent probes to determine the rate-limiting step of OGC BC activity are attempted and proposed.

Understanding the Kinetic and Thermodynamic Properties of the Thermophilic Oxoglutarate Carboxylase

By
Lucas Bruce Dillard

A thesis submitted to the Graduate Faculty of
North Carolina State University
in partial fulfillment of the
requirements for the degree of
Master of Science

Biochemistry

Raleigh, North Carolina
2019

APPROVED BY:

_____	_____
Dr. Robert B. Rose Committee Chair	Dr. Guozhu Xu
_____	
Dr. Amy Grunden	

DEDICATION

I would like to dedicate this thesis to my mother, Sherrie, and to Catie, for their unending support. Without them, none of this would be possible.

BIOGRAPHY

Lucas Dillard was born in Asheville, NC and raised by his mother, Sherrie. From a young age, Lucas showed an interest in science and technology, and with the encouragement and aid of his stepfather, Randy, was even able to win a science fair in grade school. Upon graduation from high school, Lucas attended North Carolina State University, where he was fortunate enough to find a work-study position in the laboratory of Dr. Robert Rose. While an undergraduate in the Rose lab, Lucas worked towards crystallizing the carboxyl transferase domain of oxoglutarate carboxylase and continued his work with oxoglutarate carboxylase throughout his graduate career.

TABLE OF CONTENTS

LIST OF TABLES v
LIST OF FIGURES vi

CHAPTER 1. Literature Review 1
Abstract 2
1.1. Introduction 3
1.1.1. Oxoglutarate Carboxylase 3
1.1.2. Biotin Dependent Carboxylases 2
1.1.3. Structure of the OGC BC Domain 4
1.1.4. Mechanism of the Biotin Carboxylases 5
1.1.5. Kinetic Measurements of BC Domains 6
1.1.6. OGC as a Novel Carbon Fixing Enzyme 7

CHAPTER 2. Characterization of the OGC BC Domain 10
2.1. Background 11
2.1.1. Activity of Biotin Carboxylase Domains 12
2.1.2. ATPase Assays 13
2.2. Methods 13
2.2.1. Expression and Purification 13
2.2.2. Measurement of BC Concentrations 14
2.2.3. Size Exclusion 15
2.2.4. Circular Dichroism Temperature Melting 15
2.2.5. SYPRO Orange Stability Assay 15
2.2.6. Measurement of Activity via Coupled Activity 16
2.2.7. Measurement of Activity via Discontinuous Assay 16
2.2.8. Fluorescence Measurements at Equilibrium 20
2.2.9. Stopped Flow Fluorometry 20
2.3. Results 21
2.3.1. Purification of OGC BC 21
2.3.2. Stability Measurements 21
2.3.3. Kinetics 24
2.3.4. Thermodynamic Measurements 25
2.3.5. Fluorescence Measurements 27
2.4. Discussion 29
2.4.1. Size Exclusion and Thermostability 29
2.4.2. Thermodynamic Inferences 30
2.4.3. Interpreting Fluorescence Measurements 31
2.4.4. Future Experiments 32
2.5. Conclusion 33
2.6. References 35

LIST OF TABLES

CHAPTER 2. Characterization of the OGC BC Domain

Table 2-1. Calculated parameters of OGC BC activity and energy of activation, and reported parameters of the mesophilic ACC BC, by Brett Lord..... 27

LIST OF FIGURES

CHAPTER 1. Literature Review

Figure 1-1. Cartoon diagram of an unbound OGC BC domain provided by Dr. Gregory Burhman. Domain A is shown in red, Domain B is shown in green. The T-loop of Domain B is shown in Yellow. Domain C is in Blue. (Right) OGC BC bound to ADP 5
Figure 1-2. Proposed mechanism of the BC domains. Bicarbonate stimulates degradation of ATP to produce carboxyphosphate. A biotin enolate is formed that attacks the carboxyphosphate intermediate that results in carboxybiotin. 6

CHAPTER 2. Characterization of the OGC BC Domain

Figure 2-1. Standard curve of known ATP concentrations and their corresponding peak areas as calculated by EMPOWER software 18
Figure 2-2. (Left) Purification profile of OGC BC up to elution off of Ni-NTA affinity column. (Right) Size exclusion chromatogram of OGC BC elution on 26/60 sephacryl s-300 column. 21
Figure 2-3. SYPRO Stability assays of OGC BC size exclusion peaks. (Top) Stability assay of the oligomer peak showing several dissociation steps followed by unfolding at 81°C . (Bottom) Stability assay of the dimer peak, which lacks the dissociation steps seen in the oligomer peak.……22
Figure 2-4. Circular Dichroism spectra observed from 220 nm to 280 nm at 25°C, 60 °C, 75 °C, 80 °C, and 85°C. T_m was observed to be 79°C. 23
Figure 2-5. ATP concentration vs OGC BC activity measured from 49 °C to 76 °C. Data points represent experimental velocities and their errors. Solid lines represent best fit models of the data. The error in activity measurements increased along with temperature, and analysis of enzyme negative controls suggested an increase in non-enzymatic ATP hydrolysis with temperature..... 24
Figure 2-6. Michaelis-Menten plot of biotin concentration and resulting OGC BC activity. Activity was measured via discontinuous assay at 50 °C..... 25
Figure 2-7. (Top) Emission spectra of OGC BC following excitation at 275 nm. (Bottom) Binding curve of ATP to OGC BC made by plotting the [ATP] versus the fluorescence observed at 340 nm..... 26
Figure 2-8. Stopped-flow fluorimetry data of OGC BC fluorescence. Change occurred outside the deadtime of the instruments and a rate of change could not be measured..... 28
Figure 2-9. Cartoon diagram of the OGC BC domain. Tyrosine residues are depicted in red, tryptophan residues are in pink. There are a total of 21 tyrosine residues, and 3 tryptophan residues on the enzyme. 29

CHAPTER 1

Literature Review

Lucas Dillard

Abstract

Oxoglutarate Carboxylase is a thermophilic biotin dependent carboxylase (BdC) that is unique in that it is the only known enzyme that converts 2-oxoglutarate to oxalosuccinate. Little characterization of the enzyme has been performed, yet mesophilic homologs have been extensively studied. This review focuses on the biotin carboxylase (BC) domain of these enzymes which will later be of importance in the experimental section of this thesis. Among the many families of BdCs, the BC domain remains similar in both sequence and structure. The BC domain is responsible for the ATP catalyzed carboxylation of biotin in BdCs. Controversy still exists over the exact mechanism of the BC domain, with two possible mechanisms for the degradation of ATP and addition of a carboxyl group to biotin proposed. Reported K_M values for ATP in BC domains range from 0.25 ± 0.05 mM to 8 mM in ACC and PC BC respectively. For biotin those values are reported as 84.8 ± 7.5 mM. Oxoglutarate is of biotechnological interest for its rate-limiting role in a condensed reverse TCA cycle developed to increase carbon fixation in oil seed crops. The reverse TCA cycle is proposed to be preferable to the Calvin-Benson cycle due to its independence of Rubisco, which is thought to be evolutionarily optimized for activity.

1.1. Introduction

1.1.1. Oxoglutarate Carboxylase

Oxoglutarate Carboxylase is a multi-subunit biotin dependent carboxylase (BdC) found only in deeply branching bacteria (Braakman *et al.*, 2014). *H. thermophilus* was discovered in 1984 and is in the order *Aquificales* –an ancient grouping of thermophilic bacteria found near hydrothermal vents and hotsprings. (Kawasumi *et al.*, 1984) OGC was Discovered in 2003 by M. Aoshima in H. thermophilus and mistaken for isocitrate dehydrogenase, but later reclassified as a "pyruvate carboxylase-like enzyme" once the enzyme was determined to be biotin dependent (Aoshima *et al.,* 2004).

Oxoglutarate Carboxylase catalyzes the conversion of 2-oxoglutarate to oxalosuccinate. Peak activity of the enzyme was determined to be between 70 and 80 °C. K_M for ATP dependent activity was 0.788 ± 0.050 mM with a k_{cat} of 31.7 ± 0.7 s^{-1} . A significant loss of this activity has been observed in OGC in mesophilic conditions. At 70 °C, activity was found to be significantly reduced a 20 °C (Aoshima *et al.,* 2006).

1.1.2. Biotin Dependent Carboxylases

As a member of the biotin dependent carboxylase family, OGC is homologous to an array of ubiquitously found enzymes such as Acetyl CoA carboxylase (ACC) (fatty acid biosynthesis), Pyruvate Carboxylase (PC) (Knowles, 1989; Menefee 2014). ACC and PC are both metabolic enzymes with roles in the tricarboxylic acid (TCA) cycle. PC is responsible for conversion of pyruvate to oxaloacetate –a key TCA cycle metabolite, while ACC is responsible for the first catalyzed step in fatty acid synthesis (Utter *et al.*, 1960; Tong, 2005). The mesophilic versions of BdCs have been well studied, yet little information exists regarding thermophilic BdCs such as OGC.

Biotin-dependent carboxylases have three main domains. First, a biotin carboxylase (BC) domain drives the carboxylation of a biotinylated lysine residue on the biotin carboxy carrier protein (BCCP domain). ATP degradation drives this reaction. The carboxy-biotinylated BCCP domain acts as a “swinging arm” that transfers the carboxy biotin from the active site of BC to the active site of the Carboxy Transferase (CT) domain of the enzyme. From here, the carboxy group from the biotinylated lysine is transferred to substrate (Maurice, *et al.,* 2007; Tong, 2005; Waldrop *et al.,*1994). Note that the chemistry of the BC domain is the same throughout all paralogs, and unsurprisingly, BC domains are high in sequence similarity, while CT domains and their varying functionalities vary greatly in sequence and feature a relatively high number of conserved residues. (Menefee *et al.,*2014). The first structure of a biotin dependent carboxylase was reported by Waldrop et al. in 1994 (Waldrop *et al.* 1994).

1.1.3. Structure of the OGC BC Domain

OGC BC is a Biotin Carboxylase enzyme that is a member of the ATP grasp superfamily. ATP grasp enzymes consist of an α-β fold that clasps nucleotide, and consist of three domains, A-C, that form from N to C terminus respectively (Fawaz *et al.*, 2011). However, in BCs, the C domain is separated into two subdomains, with the C_1 subdomain (also called the N-domain) at the N-terminus, and the C_2 subdomain at the C-terminus (Figure 1-1) (Wang *et al.,* 1998).

The flexible B-domain has been demonstrated to show large conformational changes through observation of apo and bound crystal structures, as well as *in vitro* experiments involving formycin ATP (FTP) (Geeves *et al.* 1995). The B-domain (residues

135-200) is highly mobile in the absence of nucleotide. Interactions with the nucleotide stabilize the B-domain in a closed conformation) (Thoden *et al.,* 2000)

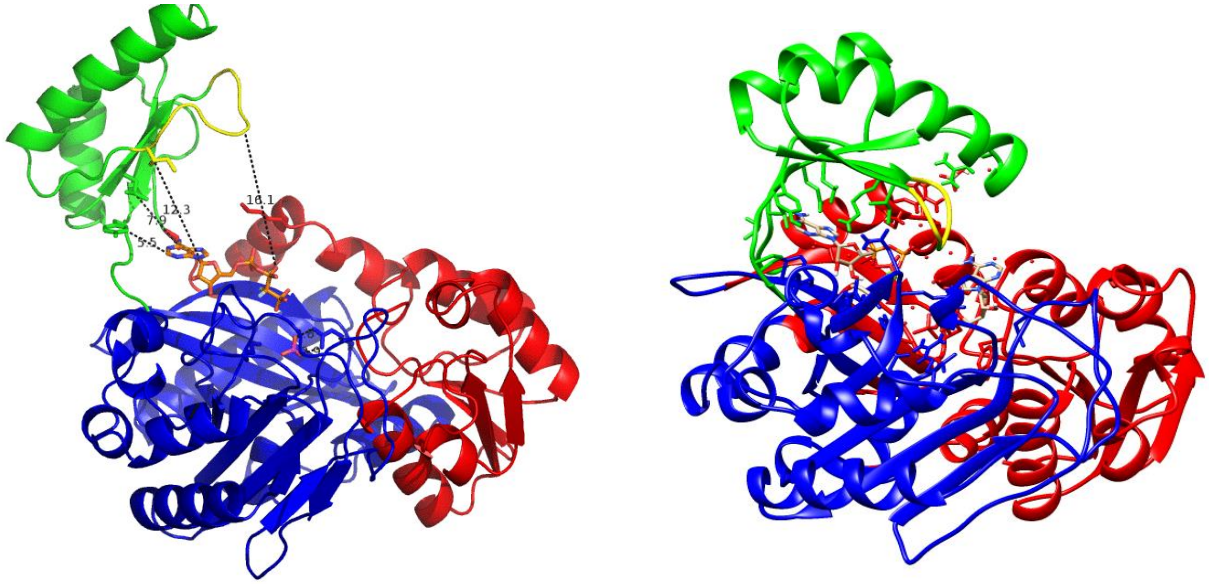

Figure 1-1. (Left) Cartoon diagram of an unbound OGC BC domain provided by Dr. Gregory Burhman. Domain A is shown in red, Domain B is shown in green. The T-loop of Domain B is shown in Yellow. Domain C is in Blue. Dashed lines correspond to distances observed between the core and B-Domain. (Right) Closed structure of the OGC BC domain with ADP in the active site.

1.1.4. Mechanism of Biotin Carboxylases

Biotin carboxylases catalyze the ATP-dependent carboxylation of biotin as shown in Figure 2. (Menefee *et al.* 2014). In this two-step reaction, bicarbonate leads nucleophilic attack on the γ-phosphate of ATP to generate a highly reactive carboxyphosphate intermediate that degrades into phosphate and carbon dioxide. The CO_2 is attacked by 1'N-2'C π-bond electrons of the enolate biotin. This nucleophilic attack leads to the creation of a carboxybiotin –the final product of the BC catalyzed reaction. A

second proposed mechanism involves the production of a O-phosphobiotin intermediate that reacts with bicarbonate to create the carboxybiotin product (Knowles, 1989). Inverse deuterium isoptopic effects have been observed in BC domains and have been understood as participation of a low-barrier hydrogen bond participating in hydrogen tunneling in the intermediate step (Lord, 2003; Levert *et al.,* 2000).

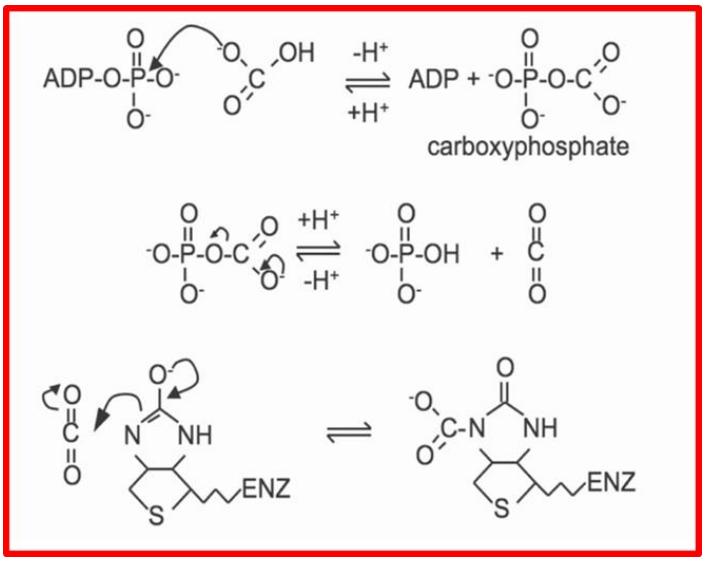

Figure 1-2. A proposed mechanism of the BC domains. Bicarbonate stimulates degradation of ATP to produce carboxyphosphate which then degrades into CO_2 and phosphate.. A biotin enolate is formed that attacks the carbon dioxide intermediate that results in carboxybiotin. (Jitrapakdee *et al.*, 2008).

1.1.5. Kinetic measurements of Biotin Carboxylases

OGC BC is capable of utilizing free biotin in lieu of BCCP –a characteristic shared only with ACC BC among BdC family members (. To date, no measurement of OGC BC activity has been achieved, but the activity of many BdCs and their domains have been characterized. Initial measurements of activity performed with respect to free biotin

concentrations reported a K_M of 111.5 ± 16.1 mM in ACC BC. The K_M of ATP for the ACC BC domain was also reported as approximately 0.6 mM (Lord, 2003).

Presence of biotin in experiments involving PC resulted in a large increase in ATPase activity . An nearly 8000 fold increase in ATPase activity was shown in ACC BC in the presence of biotin which is expected to be the result of biotin ordering nucleotide binding in the active site through substrate induced synergism. Presence of the BCCP domain has been demonstrated to increase activity of the ACC BC domain from 63.0 ± 2.8 to 1000.8 ± 182.0 min^{1}. This is thought to be because the biotinylated lysine residue of the BCCP domain reduces the number of possible conformations that the substrate may adopt in the active site of the BC domain, and reduce the off rate of substrate in the reaction (Blanchard *et al.,* 1998; Mochalkin *et al.,.* 2008). The K_M for bicarbonate for the PC BC domain was reported as 3.4 ± 1.3 mM (Attwood *et al.,* 1992).

Measurements of conformational changes experienced by the B-domain of PC were performed by Geeves *et. al.* using formycin triphosphate (FTP) –a fluorescent ATP anaolg. An FTP binding rate of 112 ± 7 s^{-1} was observed, along with a lid closure rate of 0.44 ± 0.02 s^{-1} Large changes in conformation are observed in the B-domain of apo and are consistent with the conformational changes observed in apo andbound BC crystal structures of the ACC BC domain (Geeves *et al.,* 1995; Thoden *et al.*, 2000).

1.1.6. OGC as a Novel Carbon Fixing Enzyme

Crop growth is increasingly limited on plant biology as opposed to factors such as fertilization, irrigation, and other abiotic factors (Bar Even *et. al.* 2010). Plants use the Calvin-Benson cycle to fix carbon dioxide, but the abundant enzyme ribulose 1,5 bis-

phosphate carboxylase is a bottleneck in that pathway. This is due in part to the involvement of Rubisco in photorespiration. Rubisco functions as a promiscuous enzyme that will display competitive binding of oxygen (Long *et al.,* 2006). RuBisCo is thought to be evolutionarily optimized for activity. Mutations resulting in higher turnover rates have been associated with loss of CO_2 specificity (Sage *et al.,* 2002). Accessibility of dissolved carbon dioxide relative to Rubisco has been demonstrated to be one of the limiting factors in turnover rates, with cyanobacteria even developing mechanisms of concentrating CO_2 around the enzyme (Hanson *et al*., 2016).

Attempts to circumvent the Calvin-Benson cycle and engineer plants with higher rates of carbon fixation have been attempted over the past two decades. The Calvin-Benson cycle is far from the only carbon fixing pathway, and recent years have seen an increase in the development of carbon fixing pathways for biotechnological use. Bacteria have long used alternate carbon fixing pathways, and provide a source of novel enzymes. It is thought that early bacteria utilized both the reductive and oxidative directions of the TCA cycle for energy production and carbon fixing respectively (Tang *et al.,* 2010).

A 2010 study by Bar Even *et. al.* analyzed a library of nearly 5000 carbon fixing enzymes in order to produce novel carbon fixing pathways that did not utilize RuBisCo This study performed *in silica* modeling of the carbon fixing pathways using the diverse enzyme library, and mentioned several feasible pathways –namely a condensed reverse TCA cycle. However, the author's were uncertain of the implementation of this pathway due to the oxygen sensitivity and low specific activity of OGC. This pathway was viewed a likely to improve carbon fixation rates, because it utilized bicarbonate as a

carbon source rather than atmospheric CO_2, which exists at much higher concentrations at neutral pH. (Bar-Even *et al.* 2010; Prins *et al., 1989*)

Dr. Amy Grunden proposed and implemented a modified version of the crTCA cycle into *Camelina sativa* and received a noticeable increase in oil seed yield (cite). However, Grunden cited that OGC was likely to function as a slow step in the crTCA pathway. This was thought to be because of the loss of activity OGC exhibited between its thermophilic temperature and its mesophilic temperature –an approximate 500 fold decrease in activity (Aoshima *et al.,* 2006). OGC is unique in that it is the only known carbon fixing enzyme that converts 2-oxoglutarate to oxalosuccinate. Furthermore, the enzyme is only known to exist in bacteria as a thermophilic enzyme. Thus, the characterization and normalization of OGC activity to mesophillic temperatures is of great biotechnological interest.

CHAPTER 2

Characterization of the OGC BC Domain

Lucas Dillard

2.1. Background

Net carbon emissions produced by fossil fuels have led to climate change –a defining problem of the 21st century. Biofuels derived from plant biomass have emerged as a potential fix to these decades-old problems, however, the cost of biofuels are not yet economically competitive to fossil fuels (Tao and Andy, 2009). One way to drive down the cost of biofuels is to increase the yield density of crops achieved in the field. The green revolution has had a significant impact on crop density over the past fifty years through advances in irrigation, fertilization, and pest control techniques that provide a near optimal growth environment for crops. Plant biology –specifically the rate of carbon fixation –now seems to be the limiting factor that affects crop yields. There have been studies to suggest that the Calvin-Benson carbon fixing enzyme ribulose bisphosphate carboxylase (Rubisco) has already been evolutionarily optimized for activity, and that dissolved CO_2 concentrations in the cell are positively correlated to plant growth (Bar-Even *et al.,* 2010).

The enzyme oxoglutarate carboxylase (OGC) is a weak link in the crTCA cycle with a specific activity hundreds of times slower than that of its counterparts. OGC was discovered in the bacteria *Hydrogenobacter thermophilus* in Japanese hot springs and was determined to have peak enzymatic activity at approximately 70°C, which qualifies the enzyme as a thermophile (Szilagy *et al.,* 2000). The high specific activity of OGC at 70°C is lost at mesophilic temperatures observed in field settings, thus the overarching goal of our research is to introduce mutations to OGC that would produce a 2-oxoglutarate carboxylase with high mesophilic activity. Ideally, the availability of a more active OGC would result in a more productive crTCA cycle.

2.1.1. Activity of Biotin Carboxylase Domains

The OGC BC domain is one of a handful of Biotin Carboxylase domains that can utilize free biotin as a substrate). The ATPase activity of these enzymes are greatly improved by the presence of the BCCP domain, which is thought to help order ATP in the active site via a process called “substrate induced synergism” (Mochalkin *et al.*, 2008).. Crystal structures produced by Burhman and Enrique *et al*. (in production) have shown that ADP will exist in multiple conformations within the OGC BC active site further supporting this theory.

Mutations to increase activity will target increases in the rate limiting step of the reaction. Transition state theory dictates that the rate limiting step of the reaction represents the highest energy difference between the ground and transition state of a reaction (Eyring, 1935; Peterson, 2000). This was mathematically described by Henry Eyring in 1935 via the Eyring equation, represented in Equation 1. The Eyring equation shows the relationship between the enthalpy and entropy of activation for a reaction, to the temperature dependence of the catalytic rate (k_{cat}).

$$k_{cat} = \frac{k_B T}{h} e^{\frac{\Delta S^{\ddagger}}{R} - \frac{\Delta H^{\ddagger}}{RT}} \qquad (1)$$

Determination of the rate limiting step is dependent on characterizing the temperature dependent kinetics of OGC BC catalysis. During catalysis, the B-domain of OGC BC closes over the active site to catalyze the reaction, which involves the conversion of ATP to ADP (Knowles, 1989). We have chosen to measure the rate of ATP conversion to ADP as described by the first step of the reaction in Fig. 1-2.

2.1.2. ATPase Assays

Two common assays used to measure ATPase activity are the pyruvate kinase (PK)/ lactate dehydrogenase (LDH) coupled assay, and the Malachite Green colorimetric assay. The PK/LDH assay is not capable of measuring activity at temperatures above 50 °C, as the enzymes are not thermostable (Roskoski, 1983). The malachite green assay, relies on the production of a green color change when malachite green dye is in contact with inorganic phosphate (Geledopoulos, 1991). Unfortunately, the production of non-enzymatic ATP hydrolysis at high temperatures led to high error in the malachite green assay. Because of the shortfalls of the two ATPase assays, a novel approach to measuring activity was required and developed during the research presented in this dissertation along with the resulting activity and thermodynamic parameters measured for the OGC BC domain.

2.2. Methods

2.2.1. Expression and Purification

OGC BC was expressed in BL21 (DE3*) cells. Cultures were grown in standard Lauria Broth (LB) at 37°C shaker to an optical density value of 0.6, and then induced with 1 mM IPTG. Cultures were grown overnight at 22°C. The next day cell were pelleted by centrifugation at 5,000 rpm for 10 minutes and frozen at -20°C.

For purification, cell pellets were resuspended in lysis buffer (150 mM NaCl, 10 mM Tris pH 8.0), and sonicated using six 30 second cycles at 20-30 output watts. Samples were centrifuged at 10,000 rpm for 10 minutes. The supernatant was removed and incubated in batch with Ni-NTA affinity resin (Sigma) for 1 hour. The beads were

then pelleted by centrifugation at 500 rpm for 5 minutes, and the supernatant (flow through) was removed. The beads were resuspended in a wash buffer (150 mM NaCl, 20 mM immdazole, 10 mM Tris pH 8.0). This process was repeated until the supernatant tested negative for protein in a standard Bradford assay (Kruger, 2009).

Elution was performed by suspending and loading the centrifuged beads onto a gravity column, followed by elution with elution buffer (150 mM NaCl, 250 mM imidazole, 10 mM Tris pH 8.0). Progression of protein elution was monitored via the Bradford assay. Eluted OGC BC was dialyzed overnight in Lysis Buffer to remove imidazole. Purification was monitored by SDS PAGE gels.

To increase purity, a post-dialysis heat treatment of OGC BC was also performed by heating the sample to 70°C for 5 minutes to precipitate mesophilic *E.coli* proteins, followed by centrifugation at 13,000 rpm for 10 minutes. This step was followed by addition of DTT to reduce any residues that may have been oxidized in the heating step.

2.2.2. Measurement of BC Concentrations

The concentration of the dialyzed sample was measured via A_{280} absorbance on a NanoDrop 2000. The extinction coefficient was predicted by ExPASy ProtParam software, 1.3 mg/mL per 1 Absorbance unit. OGC BC was concentrated using 3,000 Dalton molecular weight cutoff centrifugal filters spun at 3,500 rpm until the desired concentration of enzyme was achieved.

2.2.3. Size Exclusion

Size Exclusion of the OGC BC domain was performed on a GE Health Sciences 26/60 S-300 sephacryl column. A flow rate of 1 ml/min was used, and sample elution was monitored via absorbance at 280 nm. Sample elution volumes were compared against elution profiles of Bio-Rad protein standards.

2.2.4. Circular Dichroism Temperature Melting

Circular dichroism spectra were measured in 150 mM NaCl and 10 mM MOPS (pH 7.6) on a PiStar spectrophotometer. Temperatures were controlled using cell peltier system, and the far-UV CD spectra was observed from 220 nm to 280 nm. Spectra were measured six times each, at 25, 60 65, 70, 75, 80, and 85 °C.

2.2.5. SYPRO Orange Stability Assay

SYPRO orange is a dye that fluoresces when exposed to hydrophobic residues, and thus, serves as an indicator of protein melting (Yeh *et al.,* 2006). SYPRO assays were performed in a Biological Systems 3700 RT-PCR in 100 µl sample volumes containing: 10x final concentration SYPRO dye, 100 mM NaCl, 10 mM MOPS pH 7.6, and 0.5 mg/mL OGC BC. Reactions were heated in 1°C increments starting at 20°C and ending at 98°C, with fluorescence measurements taken after every degree increase in temperature. The SYPRO dye exhibits a consistent increase in fluorescence with temperature as the protein unfolds. Data was processed by plotting the temperature of each measurement versus the first derivative of the change in fluorescence with time. The T_m is the temperature associated with the peak of the derivative curve.

2.2.6. Measurement of Activity via Coupled Assay

Preliminary tests for OGC BC ATPase activity were performed via a coupled assay which involved pyruvate kinase (PK) and lactate dehydrogenase (LDH). In the coupled assay, PK uses the ADP generated by ATP hydrolysis, as well as, phosphoenolpyruvate to generate Pyruvate and ATP. The pyruvate is then utilized alongside NADH by LDH and converted to NAD^+ and Lactate (Roskoski *et al.*, 1983). The PK/LDH assay allows for spectroscopic observation of ATPase activity at 340 nm – the wavelength at which NADH absorbs and NAD+ does not absorb.

Coupled assay reagent concentrations were as follows: 100 mM NaCl, 10 mM MOPS (pH 7.6), 12.5 mM $MgCl_2$, 50 mM $NaHCO_3$, 0.2 mM NADH, 0.2 mM PEP, 10 µM PK/LDH, 41 µM Biotin, and between 0.4 and 1.1 µM OGC BC. 1 mL aliquots were placed in a Cary 1000 Spectrophotometer, and reactions were started by adding ATP at various concentrations. PK/LDH activity was verified via the use of ADP as a starting reagent. A standard curve was generated for the change in NADH absorbance versus ADP concentration.

2.2.7. Measurement of Activity via Discontinuous Assay

ATP concentration dependent activity at thermophilic temperatures (49 °C to 76 °C) was performed by a discontinuous assay, and ATPase activity was monitored via separation and quantification of both ATP and ADP using reversed phase HPLC. The assay was performed using the following final constant reagent concentrations: 150 mM NaCl, 10 mM MOPS (pH 7.6), 12.5 mM $MgCl_2$, 50 mM $NaHCO_3^-$, 41 mM Biotin. ATP concentrations were varied from 50 mM down to 0.16 mM final concentrations in 8 well

PCR strips (see results), and OGC concentrations were varied with temperature as follows: 900 nM at 49°C, 600 nM at both 58 and 68 °C, and 450 nM at 76°C.

The assay was carried out in 9-place PCR strips. A 12 mL master mix was mixed for each run with the reagent concentrations and pipetted in 100 uL aliquots to 9 of the PCR strips (a total of 72 wells). This allowed for the collection of three timepoints in triplicate (3 strips/timepoint x 3 timepoints). Three other strips were aliquoted with a no enzyme control for non-enzymatic ATP hydrolysis and represented timepoints corresponding to the experimental strips.

Timing of the quenching steps in the assays were varied with temperature to compensate with the increase in activity seen from 49 to 76 °C. These intervals were: 10, 20, and 30 minutes for assays performed at 49 °C. 7, 14, and 21 minutes for assays performed at 58 and 68 °C. 3, 6, and 9 minutes for assays performed at 76 °C. Time points were not varied with different concentrations. The strips were placed on a thermocycler block set to 4 °C, and the reaction was started by moving the strips to a second thermocycler block preheated to each respective temperature. Timepoints were taken by moving the samples from the heated thermocycler block, back to the 4 °C blocks. Note that OGC is inactive at 4 °C, and that this effectively acted as a temporary quench of the reaction. Once the samples were chilled, 80 µL of reaction volume were removed and mixed with a 20 µL volume of 0.5 M EDTA that was aliquoted into a PCR plate. The EDTA chelates Mg^{2+} ions in solution and prevents further ATP binding to OGC BC (Burke *et al.,* 1973).

Quantification of ATP and ADP was performed via phase separation on a Waters Acquity H-Class UPLC using a Pharmacia 4.6 mm x 150 mm 5 micron C_{18} reversed phase column with a 100 mM sodium monophosphate (pH 6.0) mobile phase (citation). An isocratic flow rate of 0.85 mL/min, and column temperature of 40°C were used to achieve baseline separation. 10 µl of each sample was injected and the elution profile was monitored by UV absorption at 254 nm. The integrated area of the ATP and ADP peaks were determined by the Empower software and compared to a standard curve for conversion of chromatogram data to concentrations. The standard curve was generated by injecting known concentrations of ATP or ADP and measuring the area of the resulting peaks. Concentrations were processed by converting peak areas to ATP quantities via the standard curve shown in Fig. 2-1.

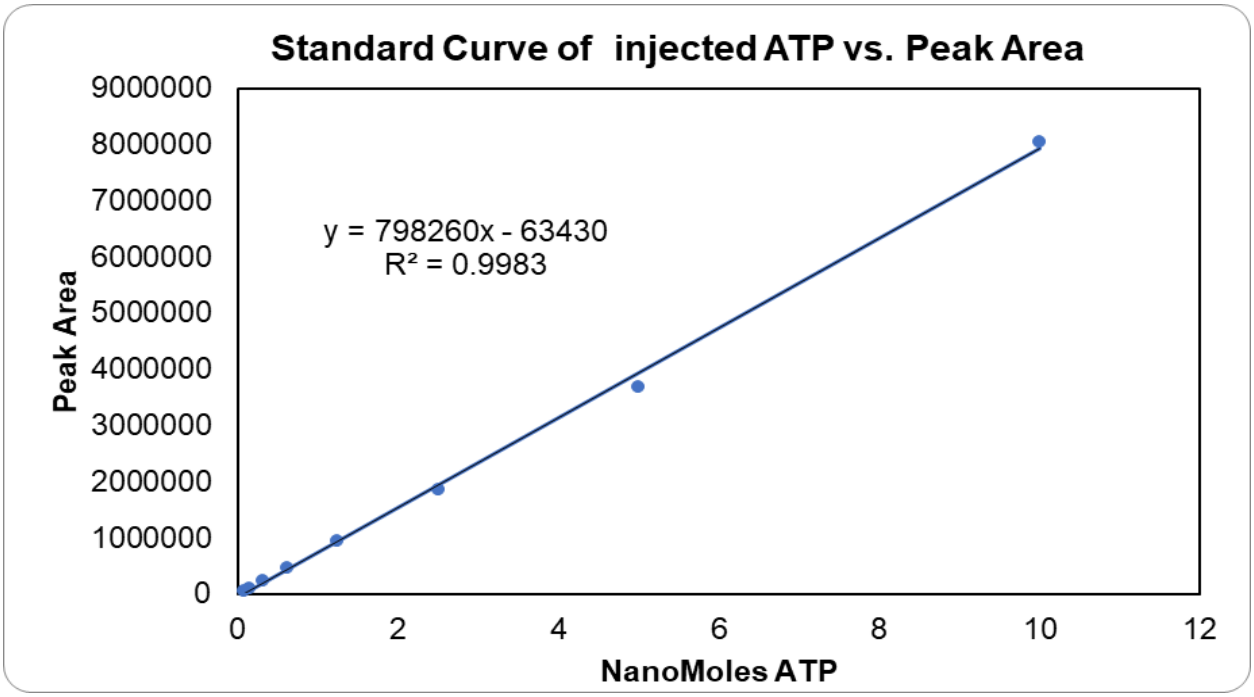

Figure 2-1. Standard curve of known ATP concentrations and their corresponding peak areas as calculated by EMPOWER software.

Timepoints and concentrations were averaged together in triplicate using the LINEST function, which used respective concentration and timepoint input to produce slope (velocity) and corresponding error values.

Michaelis-Menten plots were generated in MINITAB 18 statistical software, which produced a line of best fit in accordance with the Michalis-Menten equation (Equation 2), with error calculations of both K_m and V_{max}.

$$Velocity = \frac{((Vmax)[S])}{Km+[S]} \qquad (2)$$

The thermodynamic parameters for the transition state were calculated from an Eyring plot by plotting the reciprocal values of temperature versus the natural logarithm of k_{cat} divided by the temperature (Equation 3). $\Delta H^{\ddagger}$ is the enthalpy of activation which is derived from the slope of the line form of the Eyring equation. $\Delta S^{\ddagger}$ is the entropy of activation and is calculated from the y-intercept. T is temperature in Kelvin, k_B is Boltzman's constant, h is Planck's constant, and R is the gas constant. $\Delta G^{\ddagger}$ was calculated using Gibb's free energy equation at constant pressure (Equation 2).

$$Ln\left(\frac{k_{cat}}{T}\right) = \frac{-\Delta H^{\ddagger}}{R} * \frac{1}{T} + \frac{lnk_B}{h} + \frac{\Delta S^{\ddagger}}{R} \qquad (3)$$

$$\Delta G = \Delta H - T\Delta S \qquad (4)$$

Propagation of error was required to generate errors for measurements in $\Delta G^{\ddagger}$, $\Delta H^{\ddagger}$, and $\Delta S^{\ddagger}$ from the Vmax and Km derived from the Michaelis-Menten plots. This was calculated by taking the error of k_{cat} and multiplying by the first derivative of respective terms required in the Eyring and Gibb's free energy equations.

2.2.8. Fluorescence Measurements at Equilibrium

The dissociation constant of ATP binding to OGC BC was measured by fluorescence quenching of tyrosine residues as a function of ATP concentration. We proposed that the fluorescence change measured for ATP binding resulted from closing the B subdomain "lid" of OGC BC, also changed the environment of Tyr residues in the lid. OGC BC samples were prepared in a 150 mM NaCl and 10 mM Tris (pH 8.0) buffer, and ATP concentrations were titrated using 2-fold dilutions into individual samples so that the final concentration of ATP in the samples was varied from 20 mM to 0 mM. The final concentration of enzyme in each sample was 1 mg/mL (21 uM). 200 uL aliquots of each sample was placed in an Opaque 96 well fluorimetry plate. A wavelength of 275 nM was used to excite aromatic residues in the BC domain, and an emission spectrum of 300 to 400 nm was measured in a Molecular Devices 3000 spectrophotometer.

2.2.9. Stopped-Flow Fluorimetry

Stopped-Flow fluorimetry was attempted to measure the rate of fluorescence decrease as a result of ATP binding in a Bio-logic SFM-4000 stopped flow fluorimetry instrument with an excitation wavelength of 275 nM and an emission measurement at 340 nm. OGC BC (1 mg/ml) in a 150 mM NaCl 10 mM Tris (pH 8.0) buffer was mixed with 200 mM ATP and measured. In an attempt to slow the conformational change, a 25% glycerol buffer was also used to increase the viscosity of the solvent.

2.3. Results

2.3.1 Purification of OGC BC

OGC BC expressed well and was soluble following 1 mM IPTG induction at an optical density of 0.6. A size exclusion chromatogram of the OGC BC domain showed that at equilibrium, the OGC domain existed as a multimer of dimers (Fig. 2-2). Three peaks were observed at 100 mL, 120 mL, and 180 mL elution volumes. The final peak was crystallized and found to be a dimer (Buhrman & Enrique *et al., In production*), and SDS-PAGE analysis of the three peaks showed that each peak consisted of a 48 kDa protein (Fig. 2-2).

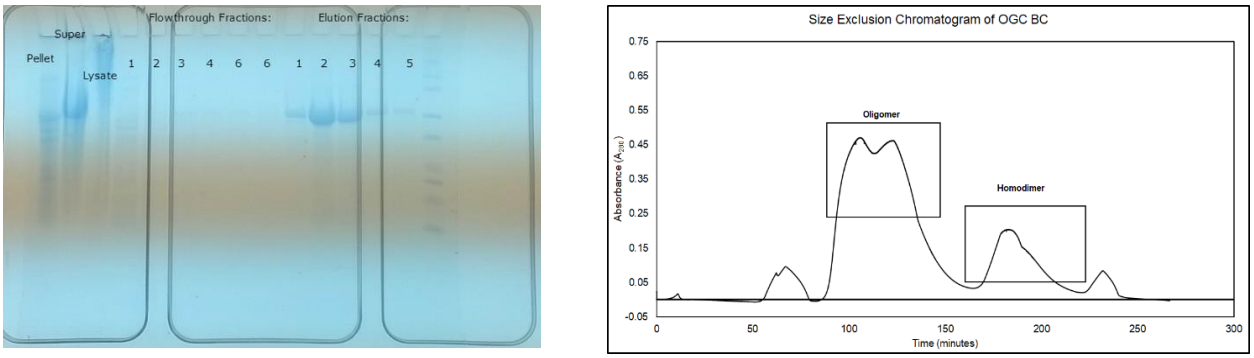

Figure 2-2. (Left) Purification profile of OGC BC up to elution off of Ni-NTA affinity column. (Right) Size exclusion chromatogram of OGC BC elution on 26/60 sephacryl s-300 column.

2.3.2 Stability Measurements

SYPRO orange stability assays of the size exclusion peaks showed varying stability of the BC aggregates (Fig. 2-3). T_m is represented by the peaks shown in the graphs. All peaks showed a final unfolding T_m of 81 °C –a result that was verified by CD (Fig. 2-4).

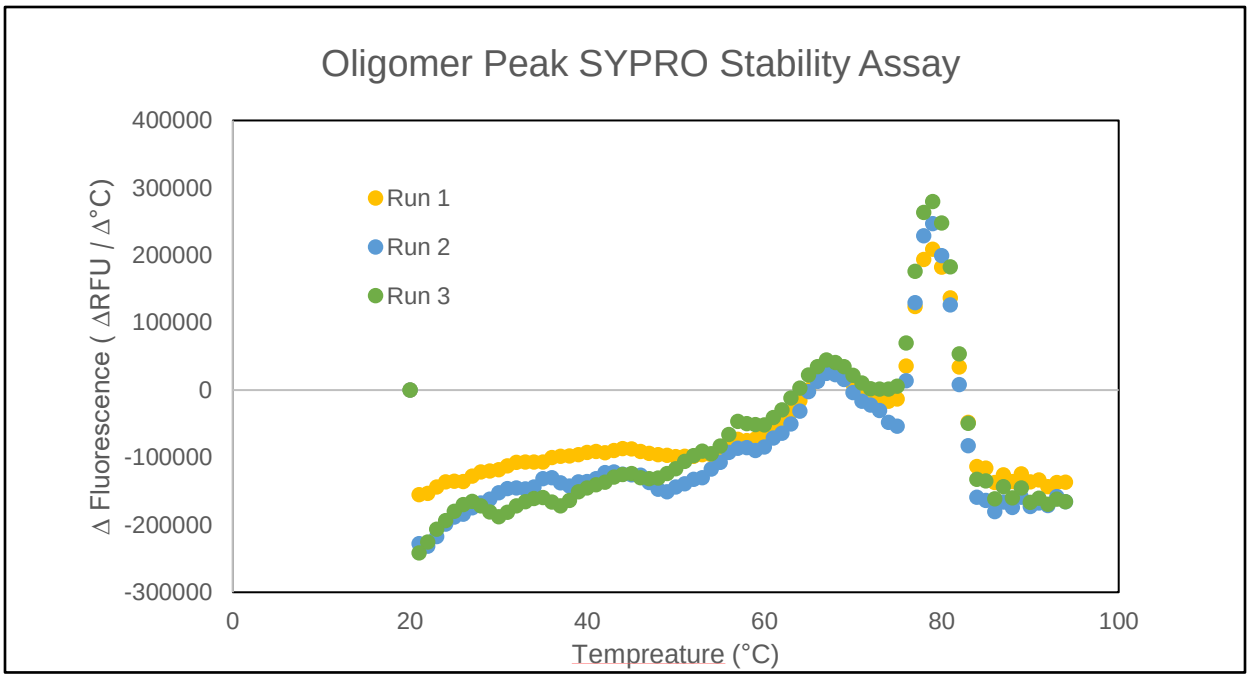

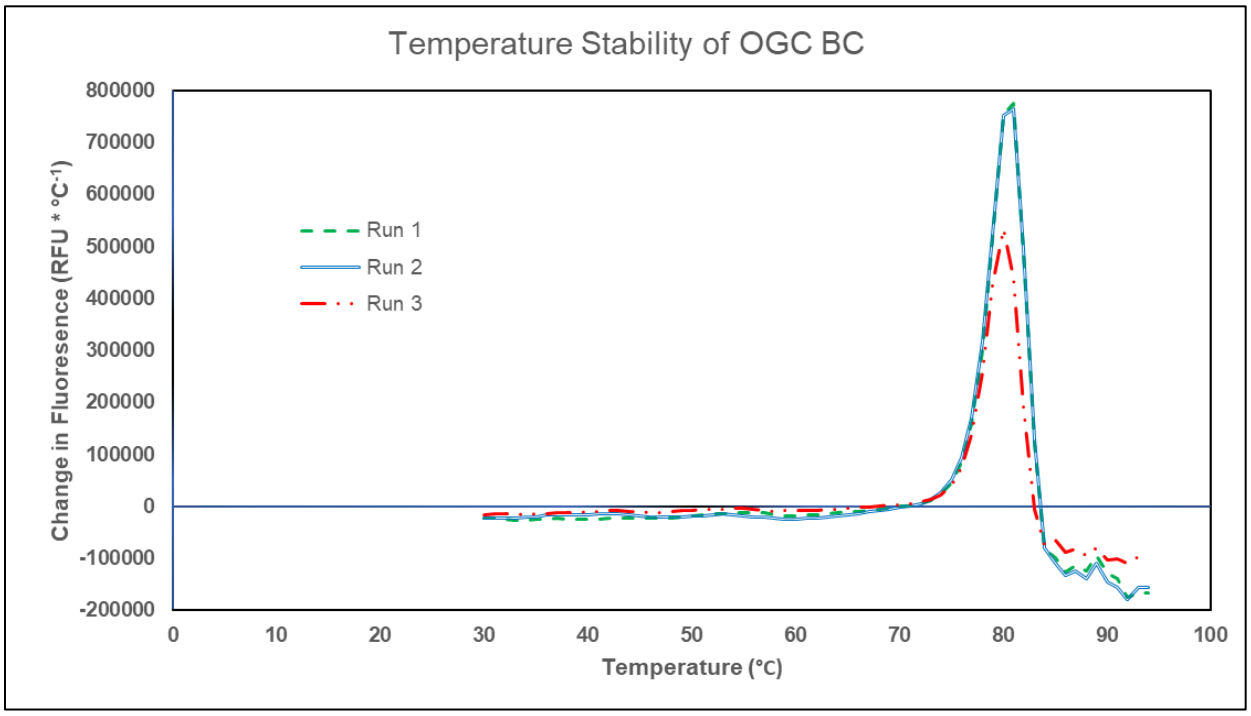

Figure 2-3. SYPRO Stability assays of OGC BC size exclusion peaks. (Top) Stability assay of the oligomer peak showing several dissociation steps followed by unfolding at 81°C . (Bottom) Stability assay of the dimer peak, which lacks the dissociation steps seen in the oligomer peak.

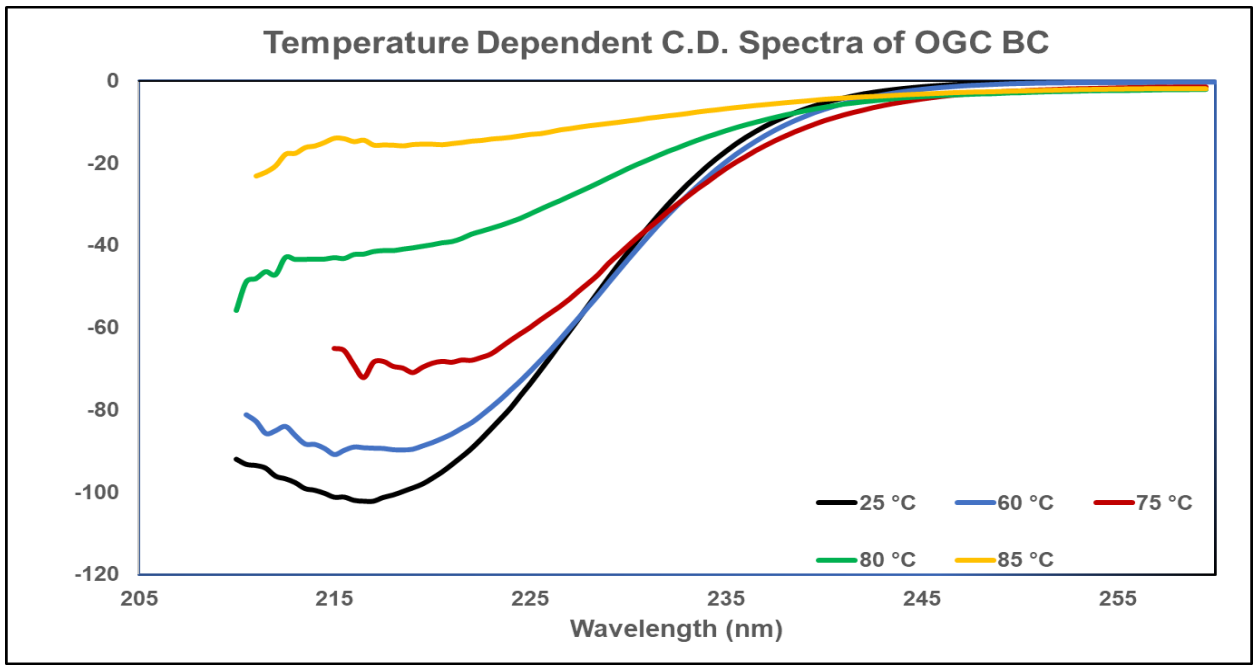

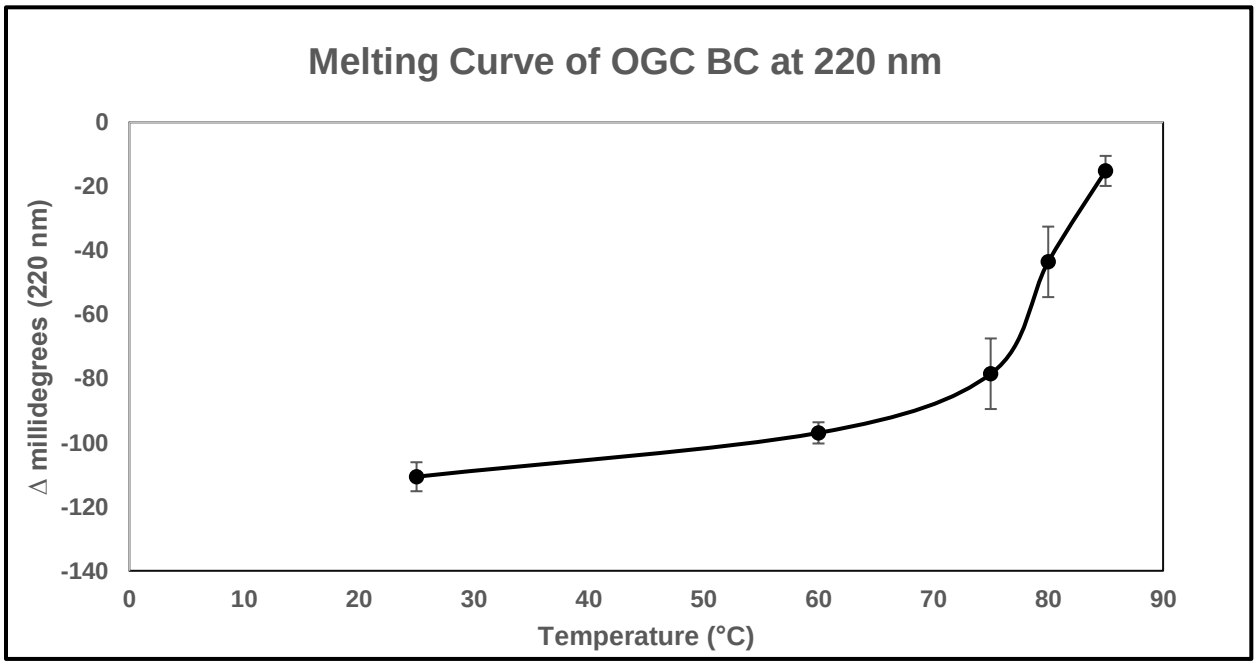

Figure 2-4. (Top) Circular Dichroism spectra observed from 220 nm to 280 nm at 25°C, 60 °C, 75 °C, 80 °C, and 85°C. T_m was observed to be 79°C. (Bottom) CD absorbance measured at 220 nm wavelength across all temperatures showing an approximate T_m of 80 °C.

Heating the aggregate peaks to 65 °C and allowing them to cool to room temperature removed the aggregate dissociation peaks from subsequent SYPRO assay data and suggested that the OGC BC aggregates are not necessarily in equilibrium.

2.3.3. Kinetics

Activity of OGC BC increased with temperature, but K_m did not significantly change from an average value of 10.91 mM. At 49 °C was 10.9 ±1.02 min^{-1}. At 58 °C k_{cat} was 30.9 ±2.49 min^{-1}. At 68 °C k_{cat} was 45.9 ±4.91 min^{-1}. At 76 °C k_{cat} was 79.2 ±12.4 min^{-1} (Fig. 2-5).

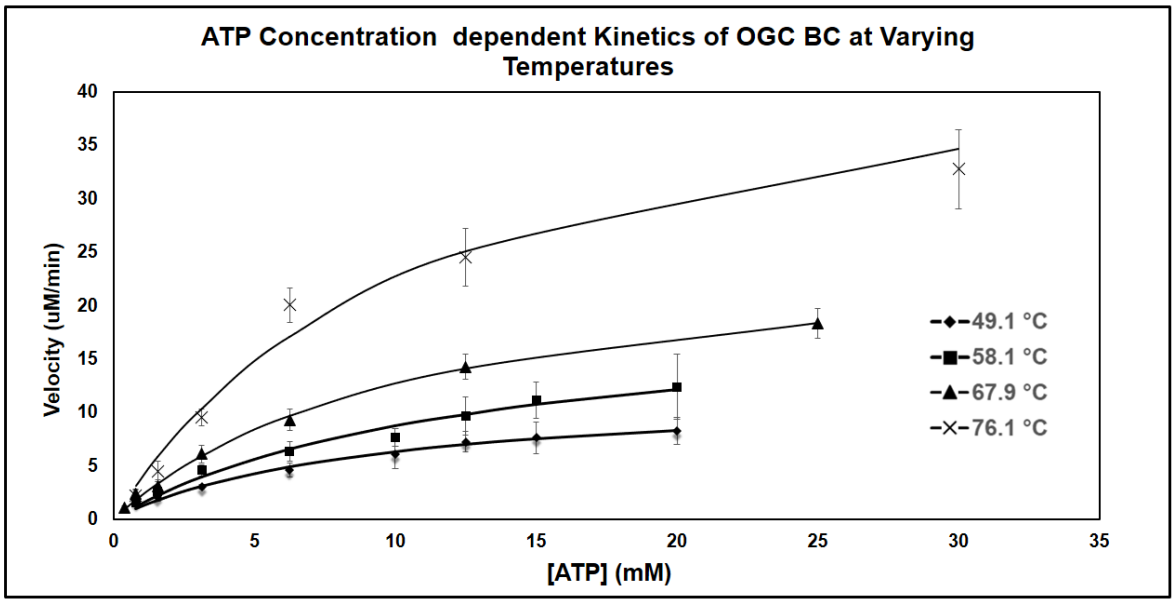

Figure 2-5. ATP concentration vs OGC BC activity measured from 49 °C to 76 °C. Data points represent experimental velocities and their errors. Solid lines represent best fit models of the data. The error in activity measurements increased along with temperature, and analysis of enzyme negative controls suggested an increase in non-enzymatic ATP hydrolysis with temperature.

ATPase activity of OGC BC was also measured in relation to varying biotin concentrations, and the K_m of biotin in this case was estimated at approximately 100 mM (Fig. 2-6). Obtaining accurate measurements in relation to biotin concentrations is difficult due to the insolubility of biotin at concentrations above 100 mM (Lord, 2003; Blanchard 1998).

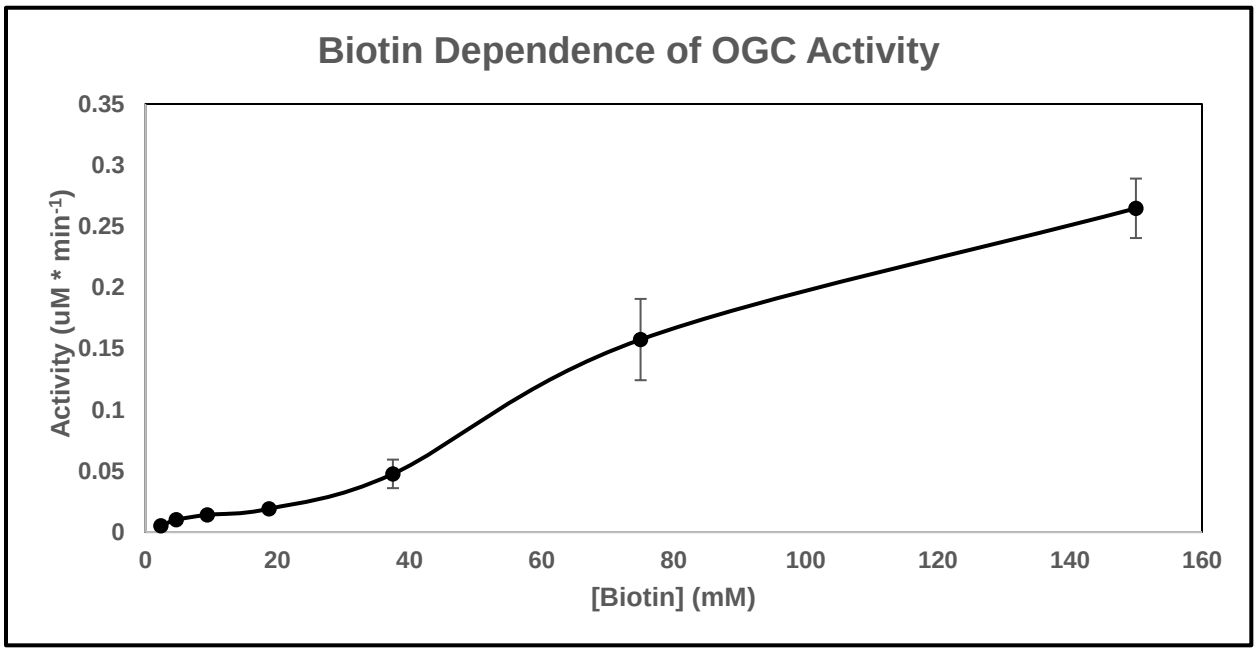

Figure 2-6. Plot of biotin concentration and resulting OGC BC activity. Activity was measured via discontinous assay at 50 °C. Bicarbonate and ATP concentrations were held constant.

2.3.4. Thermodynamic Inferences

Slope of the Eyring plot had no distinguishable changes or “breaks” that would indicate a change in rate limiting step from 49°C to 76°C (Fig. 2-7). The slope determines enthalpy of activation, which was 13.7 ± 1.3 kcal/mol. $\Delta S^{\ddagger}$ was 11 ± 4. Thus,

$\Delta G^{\ddagger}$ was calculated at 17.4 ± 1.3 kcal/mol according to equation 4 (Greiner *et al.,* 2012) at 349 K.

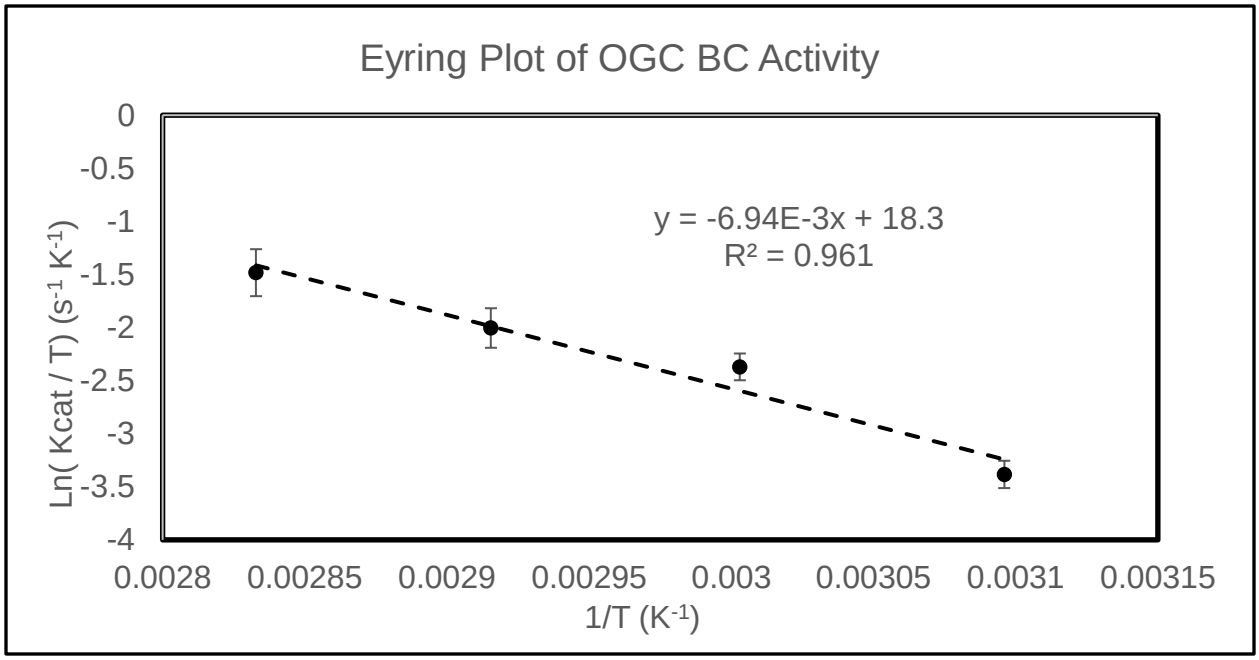

Figure 2-7. Eyring Plot of OGC BC activity calculated by plotting the reciprocal of temperature against the natural logarithm of k_{cat} divided by temperature.

Note that the value of $\Delta G^{\ddagger}$ changes very little across the measured temperature range given the low value of $\Delta S^{\ddagger}$. Values are presented in table 2-1 alongside thermodynamic values reported of the acetyl coA carboxylase BC domain –a mesophilic homolog (Lord, 2003).

Table 2-1. Calculated parameters of OGC BC activity and energy of activation, and reported parameters of the mesophilic ACC BC, by Brett Lord (Lord, 2003). Note that values for ACC BC were taken by varying biotin concentrations and observing constant bicarbonate and ATP concentrations.

Protein	**Temp (°C)**	**k_{cat}**	**K_m (mM)**	**$H^{‡}$ (kcal/mol)**	**$\Delta S^{‡}$ (cal/mol*K)**	**$\Delta G^{‡}$ (kcal/mol)**
ACC BC	50	213.5	N/A	9.54	-10.2	12.84
OGC BC	49	10.9	11	13.7 ± 1.3	11 ± 4	17.4 ± 1.3

2.3.5. Fluorescence Measurements

Fluorescence measurements taken at room temperature at equilibrium showed a gradual decrease in fluorescence with increase in ATP concentration. From this data, a K_D of ATP binding to the BC domain was found to be 1.13 mM by plotting ATP concentration ant the corresponding fluorescence of OGC BC (Fig. 2-8).

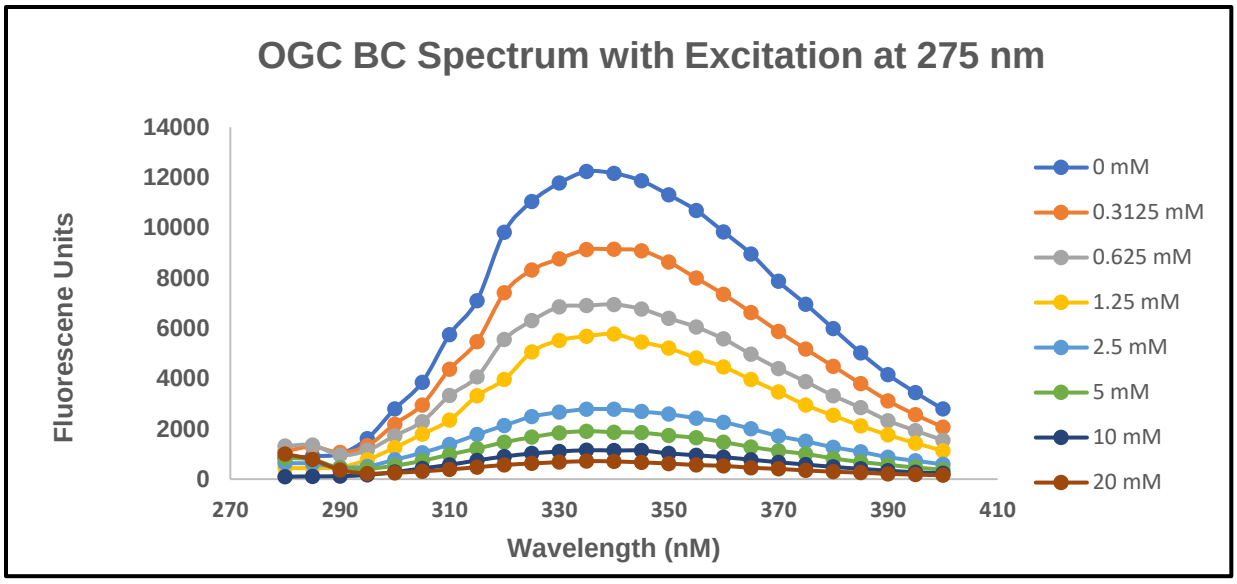

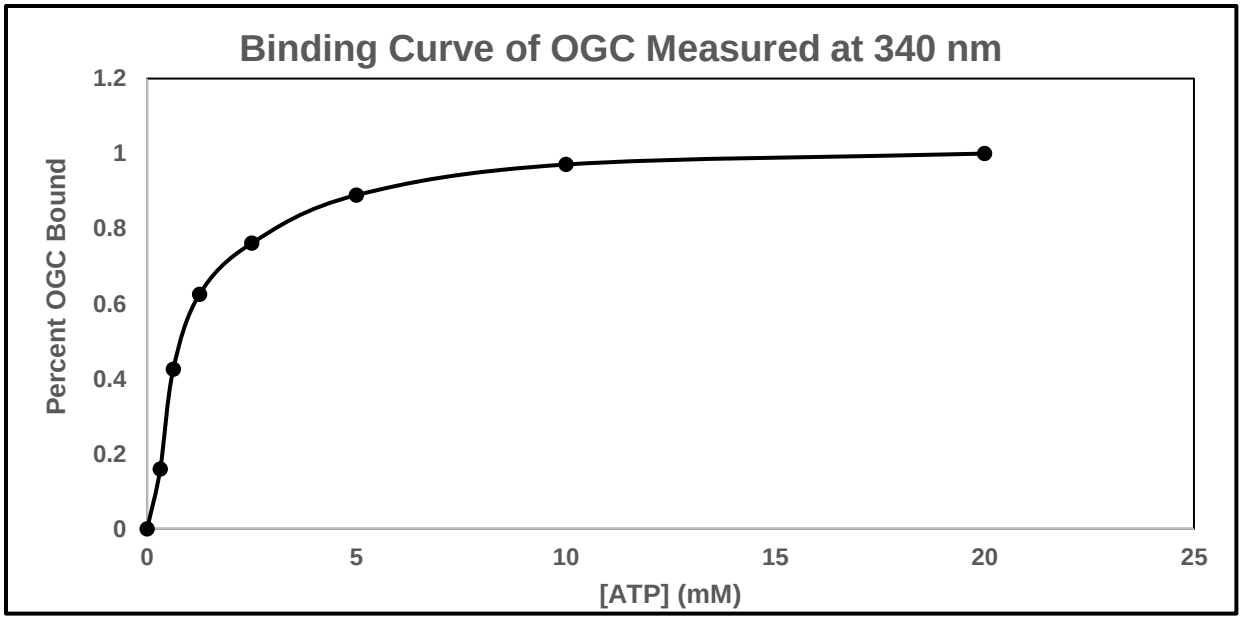

Figure 2-8. (Top) Emission spectra of OGC BC following excitation at 275 nm. (Bottom) Binding curve of ATP to OGC BC made by plotting the [ATP] versus the fluorescence observed at 340 nm.

Stopped flow fluorimetry of the OGC BC domain in the presence of ATP yielded a rate of change of at least 4000 s^{-1}. The change in fluorescence was significantly outside of the deadtime (1 ms) of the instrument, and no observable decrease in fluorescence could be observed (Figure 2-9).

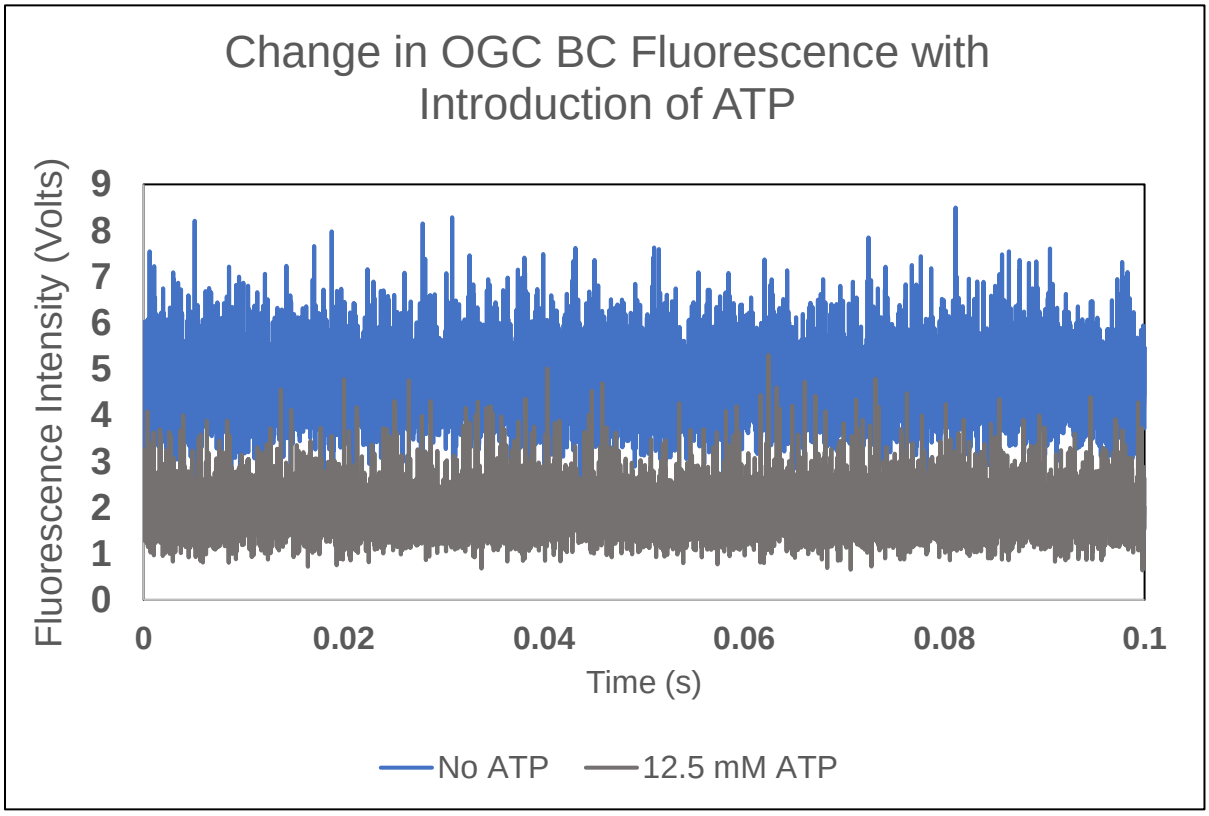

Figure 2-9. Stopped-flow fluorimetry data of OGC BC fluorescence. Change occurred outside the deadtime of the instruments and a rate of change could not be measured.

2.4. Discussion

2.4.1. Size Exclusion and Thermostability

A size exclusion and SYPRO assays both show that the BC domain exists as an aggregate of dimers. This is reinforced by increases in fluorescence observed in the larger molecular weight peaks prior to melting at 81 °C. Furthermore, in stability tests of

the OGC BC dimer peaks (Figure 2-3) no dissociation peak is observed prior to melting at 81 °C, which suggests that the unfolding of OGC BC and dimer dissociation occur simultaneously.

2.4.2. Thermodynamic Inferences

Thermodynamic values of the acetyl coA carboxylase (ACC) BC domain reported by Brett Lord were: $\Delta G^{\ddagger}$ = 12.84 ±0.64 kcal/mol, $\Delta H^{\ddagger}$ = 9.54 ±0.46 kcal/mol, and $\Delta S^{\ddagger}$ = -10.2 ±0.6 cal/mol*K (Lord, 2003). Before comparing the results of Lord, we must first consider differences between the work presented here and that of Lord. In our experiments, ATP is varied, while in Lord's work, Biotin is the varied substrate. Along with this, as described in figure 2-6, we are not observing activity at V_{max} given that our biotin concentrations were too low.

Increase in $\Delta G^{\ddagger}$ in an enzyme corresponds to a lower k_{cat} of a reaction among analogs such as, ACC and OGC (D'Amico *et al.,* 2003). Increase in the enthalpic term accounts for most of the increase in energy of activation –an intuitive result-- as one would expect an increase in stabilizing enthalpic bonds to overcome vibrational energy increases with temperature (Szilagy *et al.,* 2000).

Differences in the entropic term among ACC ad OGC BC domains were similar at -10.2 cal/mol*K and 11 cal/mol*K respectively. The enzyme conformational change and chemistry of the two domains are identical, and the reduction in degrees of freedom experienced by the substrate and lid closure from the ground state to the transition state in both the ACC and OGC BC domains are likely similar.

2.4.3. Interpreting Fluorescence Measurements

Figure 2-10 shows the tyrosine residues of OGC BC in red, and the tryptophan residues in pink. Little conformational change is seen in the core of the enzyme upon ATP binding, and the environment of the tryptophan residues is not expected to change significantly. Alternatively, the tyrosine residues in the active site were expected to see emission spectra sequestered as ATP binds in the active site.

Figure 2-10. Cartoon diagram of the OGC BC domain. Tyrosine residues are depicted in red, tryptophan residues are in pink. There are a total of 21 tyrosine residues, and 3 tryptophan residues on the enzyme.

The emission spectra exhibited by OGC BC is not consistent with a tyrosine emission spectra. Rather, a tryptophan spectra results from ATP binding, which suggests that the tyrosine residues in the active site are participating in energy transfer with the tryptophan residues outside of the binding pocket. This was confirmed by

changing the excitation spectrum from 275 nm to 300 nm. Both Trp and Tyr absorb at 275 nm. Trp absorbs at 300 nm and not Tyr does not. Trp excitation resulted in no change in the emission spectrum from ATP binding.

Measurements of OGC BC fluorescence at room temperature show a decrease in fluorescence with increasing ATP concentrations. K_d of ATP was determined to be 1.13 mM from this data. In comparison to the K_m of ATP (11 mM), K_D with respect to ATP is significantly smaller and suggests that ATP binds loosely in the active site. It is likely that we are witnessing the on-rate of ATP binding to OGC rather than lid closure.

This result is supported by the disparity between k_{cat} and stopped-flow kinetic measurements that suggest fluorescence quenching is a result of ATP binding and not closure of the OGC BC lid. Lid closure rates in other ATP binding enzymes such as adenylate kinase (Adk) have reported lid closure rates in the 100 ms timescale (Bae *et al.*, 2006). Along with this, formycin triphosphate experiments have found that the homologous PC BC domain lid closure rate is 0.44 ± 0.02 s^{-1} (Geeves *et al.* 1995, Attwood *et al.,*1992), which casts further doubt that lid closure was measured during stopped flow experiments.

2.4.4. Future Experiments

Measurement of lid closure will be performed by the addition of fluorescence resonance energy transfer (FRET) fluorophores to the lid and core of the OGC BC domain. This is advantageous because FRET measurements will provide a change in signal specifically due to lid closure instead of ATP binding. Also, the use of fluorophores with excitation spectra outside of the excitation spectra of natural aromatic

residues will prevent the energy transfer problem seen in experiments that utilized intrinsic aromatic residues.

I have already designed and cloned cysteine single mutants at sites in both the lid and the core for FRET analysis. I propose that single mutants should be probed with DTNB (also known as Ellman's Reagent) to determine the reactive rates of the mutated cysteines in each single mutant. The core/lid double mutant that creates the largest difference in the reactive rate of the lid (k_{lid}) and the reactive rate of the core (k_{core}) should be cloned and labeled with stoichiometric equivalents of fluorophore (Ratner *et al.,* 2002).

If conformational change is not rate limiting, then the deuterium isotope effect will be measured. Recall from figure 1-2, that proton transfer occurs at both steps in the OGC BC reaction. If chemistry is rate limiting due to proton transfer in one of these steps, observing the reaction in an 80% D_2O reaction buffer will affect the rate of the reaction due differences in bonding energies between deuterons and protons (Tipton and Cleland, 1988).

2.5. Conclusion

The OGC BC domain was determined to exist as a dimer that was stable to 81 °C –a result that was verified by CD and SYPRO stability assay. OGC BC was most active at 76 °C. OGC BC had an average ATP dependent K_m 10.91 mM, and the K_m with respect to biotin was approximately 100 mM. These high K_m values were consistent with those of other reported BC domains (Lord, 2003), as well as, our own crystallographic models of nucleotide binding in OGC BC.

The Eyring plot of OGC BC showed no change in slope over the range of temperatures tested, which suggests no change in rate limiting step from 49 °C to 76°C. This is important when we consider future mutations that target changes in the rate limiting step of the OGC BC reaction. FTP binding experiments in PC BC and Adk NMR studies of conformational change suggest that conformational changes in OGC BC will likely be rate limiting (Geeves *et al.,* 1995; Attwood *et al.* 1992)

Comparison to the mesophilic ACC BC, showed a larger difference in the energy of activation experienced by the thermophilic OGC BC, than in the mesophilic ACC BC at the same temperature. This difference is due to an increase in $\Delta H^{\ddagger}$, which I hypothesize is due to the need of OGC BC to form more intramolecular bonds in high energy environments.

Intrinsic fluorescence measurements proved useful in determination of K_D but stopped flow fluorimetry measurements were unsuccessful due to unwanted energy transfer between active site residues and external core residues, as well as, an uncharacteristically high binding rate that is more suggestive of ATP binding. Cysteine mutants for FRET have been designed and cloned to overcome these problems, and a proposed method for conducting these experiments was provided.

2.6. References

Aoshima, Miho, and Yasuo Igarashi. "A novel oxalosuccinate-forming enzyme involved in the reductive carboxylation of 2-oxoglutarate in Hydrogenobacter thermophilus TK-6." Molecular microbiology 62.3 (2006): 748-759.

Aoshima, M., Ishii, M., and Igarashi, Y. (2004). A novel biotin protein required for reductive carboxylation of 2-oxoglutarate by isocitrate dehydrogenase in Hydrogenobacter thermophilus TK-6. Mol Microbiol 51, 791-798.

Attwood, Paul V., and Bibiana DL A. Graneri. "Bicarbonate-dependent ATP cleavage catalysed by pyruvate carboxylase in the absence of pyruvate." Biochemical Journal 287.3 (1992): 1011-1017.

Attwood, Paul V., John H. Coates, and John C. Wallace. "Interaction of formycin A-5'-triphosphate with pyruvate carboxylase." FEBS letters 175.1 (1984): 45-50.

Bae, Euiyoung, and George N. Phillips. "Roles of static and dynamic domains in stability and catalysis of adenylate kinase." Proceedings of the National Academy of Sciences 103.7 (2006): 2132-2137.

Bar-Even, Arren, et al. "Design and analysis of synthetic carbon fixation pathways." Proceedings of the National Academy of Sciences 107.19 (2010): 8889-8894.

Blanchard, C.Z., Y.M. Lee, P.A. Frantom, and G.L. Waldrop, *Mutations at four active site residues of biotin carboxylase abolish substrate-induced synergism by biotin.* Biochemistry, 1999. **38**(11): p. 3393-400.

Blanchard, Carol Z., and Grover L. Waldrop. "Overexpression and kinetic characterization of the carboxyltransferase component of acetyl-CoA carboxylase." Journal of Biological Chemistry 273.30 (1998): 19140-19145.

Burke, Morris, Emil Reisler, and William F. Harrington. "Myosin ATP hydrolysis: a mechanism involving a magnesium chelate complex." *Proceedings of the National Academy of Sciences*70.12 (1973): 3793-3796.

D'Amico, Salvino, et al. "Activity-stability relationships in extremophilic enzymes." *Journal of Biological Chemistry*278.10 (2003): 7891-7896.

Eyring, Henry. "The activated complex in chemical reactions." *The Journal of Chemical Physics* 3.2 (1935): 107-115.

Fawaz, Maria V., Melissa E. Topper, and Steven M. Firestine. "The ATP-grasp enzymes." Bioorganic chemistry 39.5-6 (2011): 185-191

Geeves, Michael A., Joy P. Branson, and Paul V. Attwood. "Kinetics of nucleotide binding to pyruvate carboxylase." Biochemistry 34.37 (1995): 11846-11854.

Geladopoulos, Taxiarchis P., Theodore G. Sotiroudis, and Athanasios E. Evangelopoulos. "A malachite green colorimetric assay for protein phosphatase activity." *Analytical biochemistry* 192.1 (1991): 112-116.

Jitrapakdee, Sarawut, et al. "Structure, mechanism and regulation of pyruvate carboxylase." Biochemical journal 413.3 (2008): 369-387.

Knowles, Jeremy R. "The mechanism of biotin-dependent enzymes." *Annual review of biochemistry* 58.1 (1989): 195-221.

Kruger, Nicholas J. "The Bradford method for protein quantitation." *The protein protocols handbook*. Humana Press, Totowa, NJ, 2009. 17-24.

Long, Stephen P., et al. "Can improvement in photosynthesis increase crop yields?" Plant, Cell & Environment 29.3 (2006): 315-330.

Lord, Brett K. "Temperature dependent kinetics of biotin carboxylase." (2003).

Maurice, Martin St, et al. "Domain architecture of pyruvate carboxylase, a biotin-dependent multifunctional enzyme." *Science* 317.5841 (2007): 1076-1079.

Menefee, Ann L., and Tonya N. Zeczycki. "Nearly 50 years in the making: defining the catalytic mechanism of the multifunctional enzyme, pyruvate carboxylase." The FEBS journal 281.5 (2014): 1333-1354.

Mochalkin, Igor, et al. "Structural evidence for substrate-induced synergism and half-sites reactivity in biotin carboxylase." Protein Science 17.10 (2008): 1706-1718.

Peterson, George A. "Perspective on “The activated complex in chemical reactions”." *Theoretical Chemistry Accounts*. Springer, Berlin, Heidelberg, 2000. 190-195.

Prins, H. B. A., and J. T. M. Elzenga. "Bicarbonate utilization: function and mechanism." Aquatic Botany 34.1-3 (1989): 59-83.

Ratner, V., et al. "A general strategy for site-specific double labeling of globular proteins for kinetic FRET studies." Bioconjugate chemistry 13.5 (2002): 1163-1170.

Roskoski Jr, Robert. "[1] Assays of protein kinase." *Methods in enzymology*. Vol. 99. Academic Press, 1983. 3-6.

Sage, Rowan F. "Variation in the k cat of Rubisco in C3 and C4 plants and some implications for photosynthetic performance at high and low temperature." *Journal of Experimental Botany* 53.369 (2002): 609-620.

Szilágyi, András, and Péter Závodszky. "Structural differences between mesophilic, moderately thermophilic and extremely thermophilic protein subunits: results of a comprehensive survey." *Structure* 8.5 (2000): 493-504.

Tang, Kuo-Hsiang, and Robert E. Blankenship. "Both forward and reverse TCA cycles operate in green sulfur bacteria." Journal of Biological Chemistry 285.46 (2010): 35848-35854.

Tao, Ling, and Andy Aden. "The economics of current and future biofuels." In Vitro Cellular & Developmental Biology-Plant 45.3 (2009): 199-217.

Tcherkez, Guillaume GB, Graham D. Farquhar, and T. John Andrews. "Despite slow catalysis and confused substrate specificity, all ribulose bisphosphate carboxylases may be nearly perfectly optimized." Proceedings of the National Academy of Sciences 103.19 (2006): 7246-7251.

Thoden, James B., et al. "Movement of the biotin carboxylase B-domain as a result of ATP binding." *Journal of Biological Chemistry* 275.21 (2000): 16183-16190

Tipton, P.A., and Cleland, W.W. (1988) Biochemistry 27, 4325-4331.

Tong, L. "Acetyl-coenzyme A carboxylase: crucial metabolic enzyme and attractive target for drug discovery." *Cellular and Molecular Life Sciences CMLS* 62.16 (2005): 1784-1803.

Tong, Liang. "Structure and function of biotin-dependent carboxylases." *Cellular and Molecular Life Sciences* 70.5 (2013): 863-891.

Utter, Merton F., and D. Bruce Keech. "Formation of oxaloacetate from pyruvate and CO2." *Journal of Biological Chemistry* 235.5 (1960): PC17-PC18.

Waldrop, Grover L., Ivan Rayment, and Hazel M. Holden. "Three-dimensional structure of the biotin carboxylase subunit of acetyl-CoA carboxylase." Biochemistry 33.34 (1994): 10249-10256.

Wang, Weiru, et al. "X-ray crystal structure of glycinamide ribonucleotide synthetase from Escherichia coli." Biochemistry 37.45 (1998): 15647-15662.

Yeh, Andrew P., Andy McMillan, and Michael HB Stowell. "Rapid and simple protein-stability screens: application to membrane proteins." *Acta Crystallographica Section D: Biological Crystallography* 62.4 (2006): 451-457.